Acta Crystallographica Section F
Structural Biology and Crystallization Communications
ISSN 1744-3091

Crystallization and preliminary X-ray analysis of the reduced Rieske-type [2Fe–2S] ferredoxin derived from *Pseudomonas* sp. strain KKS102

Miki Senda,[a] Shinya Kishigami,[b] Shigenobu Kimura[c] and Toshiya Senda[d]*

[a]Japan Biological Information Research Center (JBIRC), Japan Biological Informatics Consortium (JBIC), 2-42 Aomi, Koto-ku, Tokyo 135-0064, Japan, [b]Graduate School of Life Science, University of Hyogo, 3-2-1 Kouto, Kamigori, Hyogo 678-1297, Japan, [c]Department of Biomolecular Functional Engineering, University of Ibaraki, 4-12-1 Nakanarusawa, Hitachi, Ibaraki 316-8511, Japan, and [d]Biological Information Research Center (BIRC), National Institute of Advanced Industrial Science and Technology (AIST), 2-42 Aomi, Koto-ku, Tokyo 135-0064, Japan

Correspondence e-mail: tsenda@jbirc.aist.go.jp

Received 14 December 2006
Accepted 2 March 2007

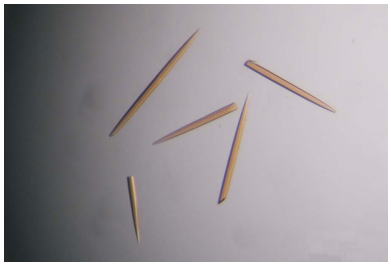

The reduced form of BphA3, a Rieske-type [2Fe–2S] ferredoxin component of the biphenyl dioxygenase BphA from *Pseudomonas* sp. strain KKS102, was crystallized by the sitting-drop vapour-diffusion method under anaerobic conditions. The crystal belongs to space group $P3_121$, with unit-cell parameters $a = b = 49.6$, $c = 171.9$ Å, and diffracts to a resolution of 1.95 Å. A molecular-replacement calculation using oxidized BphA3 as a search model yielded a satisfactory solution.

1. Introduction

BphA3 and BphA4, both derived from *Pseudomonas* sp. strain KKS102, are a Rieske-type ferredoxin and ferredoxin reductase, respectively, and comprise the electron-transfer system of the multi-component biphenyl dioxygenase BphA (Kimbara *et al.*, 1989). BphA is composed of this electron-transfer system and the terminal oxygenase BphA1A2, which catalyzes the addition of two hydroxyl groups to a benzene ring of biphenyl (Kikuchi *et al.*, 1994; Mason & Cammack, 1992) using two electrons from the electron-transfer system. The electron transfer begins with a hydride transfer from NADH to FAD in BphA4, resulting in two-electron-reduced BphA4. BphA3 then receives one electron from the reduced BphA4 and transfers the electron to BphA1A2.

In order to elucidate the molecular mechanism of the electron-transfer reaction between BphA3 and BphA4, we have studied the structure–function relationship of BphA3. Because BphA3 shuttles between BphA4 and BphA1A2, interaction between BphA3 and BphA4 should be transient; oxidized BphA3 associates with BphA4 and reduced BphA3 dissociates from BphA4. Possible redox-dependent conformational changes of BphA3 therefore seem to play a critical role in achieving an efficient electron-transfer reaction. Indeed, redox-dependent conformational changes have been observed in related ferredoxins and have been suggested to be involved in affinity regulation of the electron-donor/acceptor protein (Sevrioukova, 2005). The crystal structures of BphA3 in oxidized and reduced forms would therefore reveal the conformational changes relevant to the redox-dependent affinity regulation.

It is of note that many biological signals are transferred through transient but specific protein–protein interactions such as the BphA3–BphA4 system. Typically, their affinities are regulated by the state (ligand binding, redox *etc.*) of the proteins involved in the signalling. Understanding the molecular details of affinity regulation in biological signalling is a major challenge in current protein research. Some reports have already demonstrated such affinity regulation between signalling molecules. For example, the crystal structures of the cytochrome bc_1 complex showed two different positions for the Rieske iron–sulfur protein in the complex (Iwata *et al.*, 1998). This observation suggested that there was an affinity regulation between the Rieske iron–sulfur protein and it its redox partners, although the detailed molecular mechanism of the affinity

regulation remains unknown. To the best of our knowledge, there have been no demonstrations of the molecular mechanism of affinity regulation in biological signalling that utilize atomic resolution crystal structures, because comprehensive structural analysis of all the possible states of the signalling molecules is rather difficult.

In the BphA3–BphA4 system, the crystal structures of the electron-transfer complex between BphA3 and BphA4 and of all the redox states of BphA4, namely the hydroquinone, semiquinone and oxidized forms, have already been determined (Senda *et al.*, 2000, and unpublished results). The crystal structure of oxidized BphA3 has also been determined (Senda *et al.*, 2006). The crystal structure of reduced BphA3 is therefore the missing piece in the comprehensive structural analysis of the BphA3–BphA4 system. A comparison of the crystal structures of BphA3 in its oxidized and reduced forms would provide valuable information for understanding the redox-dependent affinity regulation between BphA3 and BphA4.

Here, we report the crystallization of reduced BphA3 under anaerobic conditions and its preliminary crystallographic analysis. Since most of the procedures for crystallization were carried out under anaerobic conditions, detailed procedures for obtaining these conditions are also described.

2. Methods and results

2.1. Anaerobic experiment

In the present study, crystallization and crystal freezing were carried out under anaerobic conditions in order to avoid the oxidation of reduced BphA3. Anaerobic conditions were prepared using an Anaerobox 'HARD' anaerobic chamber (Hirasawa; Fig. 1). The chamber was filled with a gas mixture (96% N_2, 4% H_2). Oxygen molecules in the chamber were removed using a Pd catalyst (AZX-250, Hirasawa), which catalyzes the oxidation of H_2 into H_2O using any remaining oxygen molecules in the chamber. The gas mixture was introduced for 1 min every 1 h in order to maintain anaerobic conditions. The anaerobic condition was checked with a BR0055B anaerobic indicator (Oxoido) before the experiment.

The anaerobic chamber has three rooms, one for the preparation of the protein solution and buffer, one for crystal handling equipped with a CCD microscope and one for measuring absorption spectra with a UV–Vis spectrometer. In order to carry out a controlled anaerobic experiment, we have established typical procedures that should be followed. First of all, the plasticware used for the anaerobic experiment should be stored in the chamber for more than two weeks in order to remove adsorbed oxygen molecules on its surface. Otherwise, O_2 contamination occurs. Sufficient gas exchange should be performed for the reservoir and protein solutions to remove dissolved oxygen molecules. Generally speaking, the buffers/reservoirs used for an anaerobic experiment should be kept inside the chamber for more than 24 h for further gas exchange after being bubbled with N_2 or Ar gas. All solutions were analyzed using the anaerobic indicator before use in order to ensure their anaerobic status.

Figure 1
The anaerobic chamber used in the present study. It includes a UV–Vis spectrometer (A), a microscope with CCD (B) and an incubator for crystallization (C) in the anaerobic chamber.

2.2. Protein purification and crystallization

BphA3 was overexpressed in *Escherichia coli* BL21 cells containing expression plasmid pCA3 and purified as described previously (Kimura *et al.*, 2005) under aerobic conditions. Briefly, the cells were cultured at 310 K for 30 h after induction with isopropyl β-D-thiogalactopyranoside (IPTG). The synthesized BphA3 was purified from the cells by anion-exchange and gel-filtration chromatography. The purified BphA3 was in the oxidized form, as confirmed by its absorption spectrum, which showed characteristic peaks at 460 and 590 nm (Fig. 2; Kimura *et al.*, 2005). The BphA3 was concentrated to about 12 mg ml^{-1} in 10 m*M* potassium phosphate buffer pH 7.0 containing 1 m*M* dithiothreitol and 2% glycerol. This protein solution was used for crystallization screening.

The reduction and crystallization of BphA3 were carried out in the anaerobic chamber. Concentrated BphA3 was brought into the anaerobic chamber, subjected to gas exchange in order to remove dissolved oxygen molecules and reduced as follows. BphA3 at a concentration of 11.7 mg ml^{-1} in 10 m*M* potassium phosphate buffer pH 7.0 containing 1 m*M* dithiothreitol and 2% glycerol was mixed with one equivalent of dithionite (from a stock solution of 50 m*M* dithionite), incubated for 1 h and used for crystallization screening. The reduction of BphA3 was confirmed by the absorption spectrum, which showed the two characteristic peaks of a reduced Rieske-type [2Fe–2S] cluster at 434 nm and 517 nm (Fig. 2). The initial crystallization screening was performed by the sitting-drop vapour-diffusion method using Wizard I (Emerald Biosystems) at 293 K. In addition, a series of reservoir solutions was prepared on the basis of the crystallization conditions for oxidized BphA3 and other ferredoxins.

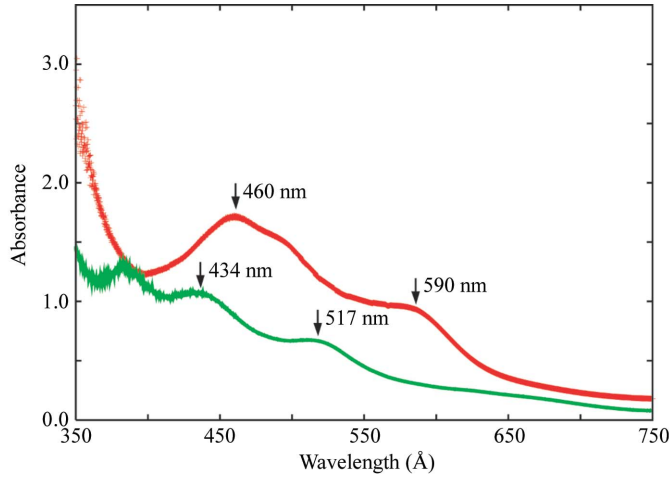

Figure 2
Absorption spectrum of BphA3 in oxidized (red) and reduced (green) forms.

Reservoir and protein solutions were degassed as described in §2.1. A sitting drop was prepared by mixing 1.0 µl each of the protein and reservoir solutions and was equilibrated against 500 µl reservoir solution. In 2 d, thin needle-shaped crystals appeared in the solution containing 2.80–2.85 *M* ammonium sulfate and 0.1 *M* imidazole pH 8.0. This condition was optimized by varying the concentration of ammonium sulfate and the incubation time of the solution containing BphA3 and dithionite, resulting in the growth of diffraction-quality crystals. For the crystallization-condition optimization, BphA3 was used at a concentration of 12.9 mg ml^{-1} in 10 m*M* potassium phosphate buffer pH 7.0 containing 1 m*M* dithiothreitol and 2% glycerol. The BphA3 solution was reduced with one equivalent of dithionite as described above. The best crystal was obtained by mixing 1.2 µl of 12.9 mg ml^{-1} BphA3 solution and 1.2 µl of an optimized reservoir solution containing 2.80 *M* ammonium sulfate and 0.1 *M* imidazole pH 8.0 at 293 K (Fig. 3). The incubation time of the BphA3–dithionite solution was 1 h. Needle-shaped crystals (approximately 0.5 × 0.03 × 0.03 mm) were obtained in 1–2 weeks.

2.3. X-ray data collection and processing

The crystals obtained were frozen using liquid nitrogen in the anaerobic chamber. The crystals were cryoprotected by soaking them in reservoir solution containing 30%(*w*/*v*) trehalose, which was degassed as described above. After 1–3 min, the crystals were flash-frozen in liquid nitrogen. The frozen crystals were stored in a dry shipper (SC 4/3V, MVE) to transport them to the synchrotron facility for data collection.

Diffraction data were collected using an ADSC Quantum 210 CCD detector at beamline NW12 of the Photon Factory-AR (PF-AR; Tsukuba, Japan; Fig. 4). The diffraction data were processed and scaled using the programs *XDS* and *XSCALE* (Kabsch, 1993). The crystals belonged to space group $P3_121$, with unit-cell parameters $a = b = 49.6$, $c = 171.9$ Å. Assuming the presence of two molecules in the asymmetric unit, the Matthews coefficient (V_M; Matthews, 1968) was calculated to be 2.6 Å^3 Da^{-1}, corresponding to a solvent content of 53%. Data-collection statistics are given in Table 1.

It is of note that auto-oxidation of the reduced BphA3 crystals under aerobic conditions for more than 2 h resulted in crystal decay, suggesting that the BphA3 in the crystal undergoes conformational changes upon oxidation. After 1 h auto-oxidation, crystals diffracted to approximately 2.7 Å resolution. The diffraction data of the auto-oxidized crystal were collected at NW12 of PF-AR (Table 1).

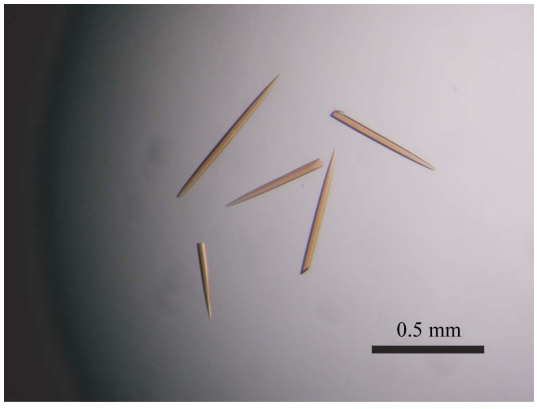

Figure 3
Crystals of the reduced form of BphA3 from *Pseudomonas* sp. strain KKS102.

Table 1
Data-collection statistics.

Values in parentheses are for the outermost resolution shell.

	Reduced BphA3	Auto-oxidized BphA3
Beamline	NW12 (PF-AR)	NW12 (PF-AR)
Crystal-to-detector distance (mm)	165.9	180.40
Oscillation angle (°)	1.0	1.0
Exposure time (s)	15.0	8.0
Wavelength (Å)	1.0000	0.9888
Space group	$P3_121$	$P3_121$
Unit-cell parameters (Å)	$a = b = 49.6$, $c = 171.9$	$a = b = 49.5$, $c = 171.2$
Resolution limits (Å)	15.0–1.95 (2.05–1.95)	15.0–2.70 (2.84–2.70)
Observations	96264	35538
Unique reflections	18629	6998
Completeness (%)	99.2 (99.9)	97.0 (97.3)
Average $I/\sigma(I)$	11.65 (5.02)	29.60 (12.26)
Redundancy	5.2 (5.3)	5.1 (5.2)
R_{merge}	0.089 (0.404)	0.035 (0.137)
Mosaicity (°)	0.245	0.136

2.4. Structure determination

The crystal structure of reduced BphA3 was determined by the molecular-replacement method using the program *MOLREP* (Vagin & Teplyakov, 1997) from the *CCP*4 program suite (Collaborative Computational Project, Number 4, 1994). The molecular-replacement calculation using the oxidized form of BphA3 (Senda *et al.*, 2006 and unpublished data) as a search model yielded a satisfactory solution. As predicted from the V_M value, the crystal contains two BphA3 molecules in the asymmetric unit. Packing analysis showed that there were no close contacts between the subunits.

The R_{iso} value between the reduced and auto-oxidized BphA3 diffraction data was 0.256 at 3 Å resolution, suggesting some conformational changes in the crystal. The (reduced − auto-oxidized) difference Fourier analysis with phases derived from the partially

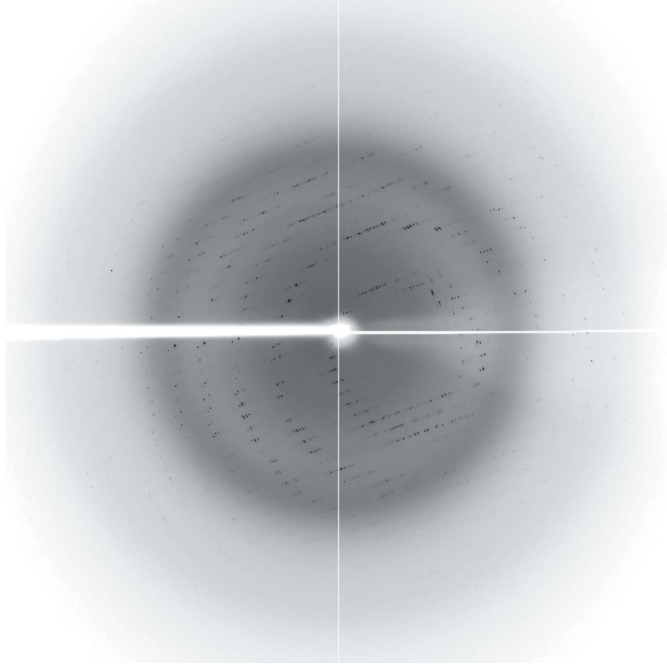

Figure 4
X-ray diffraction pattern of the reduced form of the BphA3 crystal. The diffraction data were collected at beamline NW12 of PF-AR using an ADSC Quantum 210 CCD detector.

refined structure of reduced BphA3 showed clear difference densities around the peptide bond close to the [2Fe–2S] cluster. These observations suggested that there are some structural differences between the oxidized and reduced forms of BphA3. Crystallographic refinements of reduced and auto-oxidized BphA3s at 1.95 and 2.7 Å resolution, respectively, are in progress.

We thank Professor Fukuda for his continuous support of our work. This study was supported in part by the New Energy and Trial Technology Development Organization (NEDO) of Japan.

References

Collaborative Computational Project, Number 4 (1994). *Acta Cryst.* D**50**, 760–763.
Iwata, S., Lee, J. W., Okada, K., Lee, J. K., Iwata, M., Rasmussen, B., Link, T. A., Ramaswamy, S. & Jap, B. K. (1998). *Science*, **281**, 64–71.
Kabsch, W. (1993). *J. Appl. Cryst.* **26**, 795–800.
Kikuchi, Y., Nagata, Y., Hinata, M., Kimbara, K., Fukuda, M., Yano, K. & Takagi, M. (1994). *J. Bacteriol.* **176**, 1689–1694.
Kimbara, K., Hashimoto, T., Fukuda, M., Koana, T., Takagi, M., Oishi, M. & Yano, K. (1989). *J. Bacteriol.* **171**, 2740–2747.
Kimura, S., Kikuchi, A., Senda, T., Shiro, Y. & Fukuda, M. (2005). *Biochem. J.* **388**, 869–878.
Mason, J. R. & Cammack, R. (1992). *Annu. Rev. Microbiol.* **46**, 277–305.
Matthews, B. W. (1968). *J. Mol. Biol.* **33**, 491–497.
Senda, M., Kimura, S., Kishigami, S. & Senda, T. (2006). *Acta Cryst.* F**62**, 590–592.
Senda, T., Yamada, T., Sakurai, N., Kubota, M., Nishizaki, T., Masai, E., Fukuda, M. & Mitsui, M. (2000). *J. Mol. Biol.* **304**, 397–410.
Sevrioukova, I. F. (2005). *J. Mol. Biol.* **347**, 607–621.
Vagin, A. & Teplyakov, A. (1997). *J. Appl. Cryst.* **30**, 1022–1025.